Warp Drive Constraints, Gravitational Energy Storage, and a Proposed Proper-Time-Matched Flight Experiment

Todd J. Desiato*

Independent Researcher, Statesville, North Carolina 28625, USA

Abstract

Spacetime constructs are inadmissible as independent physical propulsion agents in the matter-first description of Operational Quantum Gravity (OQG). Within its common-scale family, covariant material scaling stores reversible gravitational lifting work in increased bound-state energy measured against retained external standards. A complete isolated spacecraft and controller cannot accelerate through internal stresses in a uniform exterior; propulsion requires momentum exchange through exhaust, radiation, or external bodies. The quantum-state construction links increased rest energy to a still larger equilibrium volume, yielding lower positive rest-state energy density and faster clock transitions. Matching the material scale to the Lorentz factor gives equal proper-time rates and restores the longitudinal reference length. For radial flight in a weak external gravitational field, matching requires squared speed equal to twice the potential rise and outward thrust acceleration twice local gravity. We propose a 100 kilometer terrestrial flight experiment to test proper-time-rate matching during powered ascent and descent on the Einstein-equivalent branch. The idealized trajectory requires a 3.96182 kilometer-per-second propulsive velocity increment and predicts a 1.46937 nanosecond clock lead accumulated during ballistic turnaround. The storage relation and tracking Hamiltonian specify coordinated material-control requirements within a complete energy–momentum account.

* Independent researcher. Corresponding author: mainengineering@gmail.com. ORCID: 0000-0002-7514-0169.

Nomenclature

Symbol	Definition
$A_{2,\mathrm{E}}^{\mathrm{tot}}$	Total static spectral stiffness, J^2
E_0, E_b	Reference and prepared body rest-state energies, J
b	Common material scale factor
c_0, c_b	Reference and prepared light speeds in retained coordinates, $\mathrm{m\ s^{-1}}$
u	Comparison velocity or speed, as specified, $\mathrm{m\ s^{-1}}$
$\hbar$	Fixed reduced Planck constant, J s
γ	Lorentz factor
τ_0, τ_{s}	Reference and spacecraft proper times, s

Other nomenclature is defined within the body of the paper.

I. Introduction

Propulsion by controlled gravitational response poses two linked physical questions: where the vehicle transfers momentum, and where the work used to change its gravitational state is stored. Operational Quantum Gravity (OQG) [1, 2, 3] addresses these questions through matter and its retarded stress response. The analysis excludes spacetime constructs as independent propulsion agents within OQG, establishes the momentum requirement for a complete ship–controller system, identifies lifting work with stored bound-state energy, and derives powered trajectories whose proper-time rates match an external gravitational reference.

The Alcubierre and Natário constructions prescribe warp geometries and determine their required source stresses [4, 5], with broad classes constrained by energy-condition theorems [6]. Millis [7] identified the net external force requirement for hypothetical space drives, including the internal reaction between an onboard field generator and its vehicle. The present analysis applies that conservation foundation to OQG and connects it to a quantum-state construction, a material account of lifting work, and a proposed clock-matched flight experiment.

In OQG, clocks and rulers obtain their rates and dimensions from quantum transitions and binding. Their gravitational comparisons have an Einstein-equivalent representation in general relativity (GR) on the selected long-wavelength branch. Geometry is bookkeeping for those material intervals. A spacetime bubble or river therefore supplies no independent physical carrier of propulsion. The complete spacecraft, controller, power supply, supports, and fields carry the energy and momentum. In a uniform exterior, conservation of their symmetric total stress

excludes acceleration through internal forces alone. Exhaust, radiation, or external bodies provide the required momentum exchange; radiation-only export is bounded by ideal photon-rocket recoil.

Covariant material scaling denotes the coordinated change of bound-state energy, equilibrium dimensions, and transition frequencies. It describes a family of material states; general covariance denotes the separate freedom to choose coordinates. Within the stated OQG family, the quantum construction identifies reversible gravitational lifting work with the increase in bound-state energy measured in retained external standards. The body expands while storing that work, and its volume grows faster than its energy, reducing its positive rest-state energy density. This develops the material objective of *The Electromagnetic Quantum Vacuum Warp Drive* [8] into an explicit storage relation and coordinated spectral and binding requirements, including nuclear structure.

Matching the material scale to the Lorentz factor gives equal proper-time rates relative to the reference clock and restores the longitudinal reference length. For radial flight in the weak terrestrial field, the matching condition fixes squared speed to twice the Newtonian potential rise and outward thrust acceleration to twice local gravity. We propose a 100 km ascent-and-return flight experiment using Earth's ambient and conventional thrust. Its powered branches maintain equal clock rates relative to the ground reference; ballistic turnaround adds a 1.46937 ns lead retained at landing. The propulsive velocity increment is 3.96182 km/s. The trajectory and clock history follow the Einstein-equivalent branch, on which OQG's material-response description and GR's geometric representation give equivalent gravitational predictions.

The controller specification then translates the material result into an ideal tracking Hamiltonian and linked spectral, dimensional, density, and stress-response targets. Its complete energy–momentum budget includes the source and its structural participation. Sections II–VII establish the propulsion boundary, quantum preparation, storage relation, and adopted gravitational normalization; Sections VIII–IX give the flight calculation and controller requirements.

II. An onboard generator carries the reaction to the force it produces

A generator that pushes the spacecraft's matter must itself participate in the reaction. If the generator is mounted inside the vehicle, that reaction acts within the vehicle. A proposed free-fall propulsion mechanism must therefore be tested with the generator, its energy supply, and its fields included. The decisive quantity is the motion of this complete system.

Operational Quantum Gravity (OQG) takes the prepared state and causal stress response of Standard-Model matter as its physical foundation [1, 2, 3]. The Standard Model describes elementary matter and its electromagnetic, weak, and strong interactions. Its stress-energy tensor collects energy density, momentum transport, pressure, and shear stress. A causal response includes the time required for a disturbance to reach and change the receiving matter. Clocks and rulers participate in that response through the transitions and binding processes that determine their readings and dimensions.

The selected long-wavelength branch applies when disturbances vary over distances much larger than microscopic binding structures. Its observable gravitational comparisons have an Einstein-equivalent representation in general relativity (GR). The metric is the mathematical rule for those interval comparisons; in OQG it records the matter response. The material source and its interactions supply the physical mechanism. This ordering also identifies what an engineering design must specify: the source, the receiving matter, their coupling, and the complete transfer of energy and momentum.

Consider an isolated apparatus in a uniform exterior reference state. Include the hull, passengers, controller, power supply, supports, and interacting fields within the complete system. In an inertial reference account, let t denote time and $\mathbf{x}$ position. Let ε be total energy density, $\mathbf{S}$ energy flux, $\mathbf{g}_P$ momentum density, and σ_{ij} momentum flux. Spatial indices i,j run over three directions, repeated indices are summed, and ∂_i denotes a spatial derivative. The symbol $\nabla\cdot$ denotes divergence. With c_0 the exterior reference light speed, a symmetric conserved total stress gives

$$\partial_t \varepsilon+\nabla\cdot\mathbf{S}=0, \qquad \partial_t g_{P,i}+\partial_j \sigma_{ij}=0$$
$$\mathbf{S}=c_0^2\mathbf{g}_P \tag{1}$$

Integrate over the complete localized system, with vanishing boundary flux. Its total energy E and momentum $\mathbf{P}_{\text{tot}}$ are then constant. Define the center of energy $\mathbf{X}_E$ as the energy-weighted mean position. Integration by parts gives

$$\mathbf{X}_E=\frac{1}{E}\int \mathbf{x}\varepsilon \, \mathrm{d}^3x$$
$$\frac{\mathrm{d}\mathbf{X}_E}{\mathrm{d}t}=\frac{c_0^2\mathbf{P}_{\text{tot}}}{E}, \qquad \frac{\mathrm{d}^2\mathbf{X}_E}{\mathrm{d}t^2}=0 \tag{2}$$

The lifting interaction makes the result concrete. Partition the complete system consistently into receiving matter, a generator assembly including its power supply and supports, and their interaction fields. Denote their momenta by

$\mathbf{P}_{\text{body}}$, $\mathbf{P}_{\text{gen}}$, and $\mathbf{P}_{\text{field}}$, with each contribution counted once. Define $\mathbf{F}_{\text{body}}$ and $\mathbf{F}_{\text{gen}}$ as the rates of change of the first two momenta. For internal operation with no boundary transfer,

$$\begin{aligned} \Delta\mathbf{P}_{\text{body}}+\Delta\mathbf{P}_{\text{gen}}+\Delta\mathbf{P}_{\text{field}}&=0 \\ \mathbf{F}_{\text{body}}+\mathbf{F}_{\text{gen}}&=-\frac{\mathrm{d}\mathbf{P}_{\text{field}}}{\mathrm{d}t} \end{aligned} \tag{3}$$

When field momentum is stationary, an upward force on the receiving ship has an equal downward reaction on the generator assembly. During a transient, the fields carry the difference; over a cycle that returns them to their initial state, the material impulses are equal and opposite. If the apparatus lifts matter against an external gravitational field, the gravitating body and any external supports enter the larger reaction account as well.

The proposed source that repels receiving matter acts as an anti-gravity generator in the specific sense of controlled repulsive gravitational response. If it pushes the receiving matter away, it takes the opposing momentum. Attaching it to the ship returns that reaction through the mounts, structure, and fields. The resulting tension or compression is an internal load, whose magnitude and distribution follow from the actual interaction. Calling the repulsive motion free fall does not turn that internal load into thrust on the complete spacecraft.

Raising the body's internal energy and pushing its center of mass are distinct operations. A uniform preparation can transfer energy without selecting a direction of motion. The reaction in Eq. (3) is required whenever the generator supplies the directed lifting or repulsive force. Both operations belong in the complete source account, and neither permits momentum to be created inside the isolated vehicle.

A passenger geodesic describes unloaded motion in the equivalent geometric description; propulsion must account for the source that establishes it. Turning the generator off leaves the balance intact: released stresses, field transients, and emitted radiation carry the corresponding momentum.

The apparatus proof uses an inertial exterior and the complete symmetric stress. Strong self-gravitating systems require the corresponding total energy and momentum charges and their fluxes at large distance [9, 10]. In an external gravitational field, the external source belongs in the reaction account. These declared boundaries identify the physical domain of the exclusion.

Radiation provides an allowed momentum export. Let $E_{\mathrm{rad}}>0$ be the total outgoing radiation energy in one inertial exterior frame, and let the unit vector $\mathbf{n}$ give each element's direction. For massless radiation with momentum magnitude equal to energy divided by c_0, conservation and the triangle inequality give

$$|\Delta\mathbf{P}_{\mathrm{veh}}|=\left|\int \frac{\mathbf{n}}{c_0}\,\mathrm{d}E_{\mathrm{rad}}\right|\leq\frac{E_{\mathrm{rad}}}{c_0} \tag{4}$$

Here $\Delta\mathbf{P}_{\mathrm{veh}}$ includes the momentum change of all retained vehicle components and fields. Perfectly collimated emission reaches the bound. With $\overline{F}$ the useful mean recoil thrust and $\overline{P}_{\mathrm{rad}}$ the mean outgoing radiation power, steady operation or a completed-cycle average therefore satisfies

$$\overline{F}\leq\frac{\overline{P}_{\mathrm{rad}}}{c_0} \tag{5}$$

An isolated radiation-only controller is consequently bounded by ideal photon-rocket recoil for the same exported energy. Massive exhaust, incident beams, and forces from external bodies have different momentum accounts. Stored field momentum also distinguishes a transient component force from the completed-cycle thrust in Eq. (5). These distinctions allow the bound to be applied to a proposed mechanism using its actual boundary and energy supply.

Geometric warp constructions address an additional requirement: the source stress needed for a chosen metric. The Alcubierre and Natário constructions specify such targets [4, 5]. For the broad classes analyzed in Ref. [6], the source violates the null energy condition (NEC), and therefore also the weak (WEC), strong (SEC), and dominant (DEC) energy conditions of GR. A local renormalized energy density, measured relative to a specified vacuum subtraction, can be negative in quantum field theory. That statement concerns a local observable; the complete system governed by a Hamiltonian bounded below still has its ground-state lower bound. Quantum energy inequalities constrain the distribution and duration of negative local energy density in their applicable field and sampling regimes [11]. A negative local energy density therefore supplies neither an arbitrary macroscopic source nor permission to place the complete system below its ground state.

A positive-energy subluminal shell, including the constant-velocity examples studied in Refs. [12, 13], still requires a preparation and propulsion history. Source admissibility asks which metric comparisons an allowed material history can realize; the conservation proof asks where the complete apparatus obtains momentum. Einstein equivalence on a selected branch alone does not classify every globally allowed source history. Within the closed onboard setting, however, the momentum exclusion is definite and independent of that broader classification.

Descriptions of a spacetime bubble or river express interval relationships; they supply no additional reaction medium. In the closed onboard setting of Eq. (2), the same conservation result governs a proposed geodesic warp drive. An external generator anchored to a large body instead permits momentum exchange with that body and its fields. Such a system is an externally assisted accelerator. The external source does the lifting, as a crane would lift the ship to the top of a tall building; release then converts the stored lifting energy into motion. An onboard generator acting only between parts of the ship cannot lift the complete assembly from within. Passage through a stationary localized potential between equal-potential endpoints gives equal asymptotic kinetic energies; net energy gain requires the appropriate unequal endpoints, source motion, or time-dependent energy supply.

The material objective developed in *The Electromagnetic Quantum Vacuum Warp Drive* [8] remains a separate control question: increase the body's energy while increasing its equilibrium volume still faster, thereby lowering its positive energy density. OQG expresses that target through the complete interacting matter response. Its fixed-measure source construction also makes the local connected response independent of an arbitrary common vacuum-energy offset at fixed preparation [2, 3]. State-dependent fluctuations, binding, and boundary stresses remain part of the physical system.

The remaining onboard task is to prepare the ship's material state while an accounted propulsion system changes its motion. That preparation has a definite energy and density requirement.

III. Material scaling matches the moving clock and longitudinal length

Clock compensation requires a specific change in the spacecraft's matter. The prepared state must run its internal transitions faster by precisely the factor that motion slows the clock comparison. Its equilibrium dimensions and positive energy density must change with those transitions. Deriving these linked requirements identifies what the generator must prepare while an independently accounted propulsion system accelerates the vehicle.

Retain one observer's clock, ruler, and energy standards, called reference state 0. Compare the same material content in a settled isotropic family, with the same dimensionless proportions and probabilities of occupying corresponding quantum levels. Isotropic means that the equilibrium scale changes equally in every direction. The ambient is the surrounding physical state of matter and fields. In the small-body comparison it varies negligibly across the receiving body. One positive factor b labels this common-scale family; Sections IV–VII develop its state and response requirements.

For a material standard labeled a, let L_a be equilibrium length and ω_a its transition angular frequency. Let E_b be the body's complete rest-state energy, with reference value E_0. Let c_b be light speed expressed in the retained reference coordinates, with reference value c_0, using one declared propagation and synchronization convention. This is a comparison of light propagation using the retained standards, distinct from a shifted material resonance or a dispersive group velocity in a medium. The selected OQG family has

$$\frac{L_a}{L_{a0}}=\frac{\omega_a}{\omega_{a0}}=\frac{E_b}{E_0}=b, \qquad \frac{c_b}{c_0}=b^2 \tag{6}$$

For $b>1$, lengths and transition frequencies increase together. The dimensionless combination $\omega_a L_a/c_b$ remains fixed. Local instruments that share the scaling retain the same dimensionless mutual readings; comparison with the original external standards reveals the change. The term covariant matter scaling refers to these linked transformations. General covariance is the separate freedom to express physical laws in different coordinates.

Let τ_0 denote reference proper time, the time recorded by the reference clock, and set $t=\tau_0$. Write $\mathbf{x}_s(t)$ for the spacecraft position, $\mathbf{u}=\mathrm{d}\mathbf{x}_s/\mathrm{d}t$ for its comparison velocity, and $u=|\mathbf{u}|$ when only speed matters. The dimensionless speed β and Lorentz factor γ are

$$\beta=\frac{u}{c_b}, \qquad \gamma=(1-\beta^2)^{-1/2} \tag{7}$$

The preparation raises the rest clock rate by b, while motion contributes the familiar factor $1/\gamma$. Let τ_s be calibrated spacecraft proper time, $L_\parallel$ its longitudinal length obtained from simultaneous endpoint positions in the reference frame, and $L_\perp$ a transverse length. Applying each comparison factor once gives

$$\frac{\mathrm{d}\tau_s}{\mathrm{d}\tau_0}=\frac{L_\parallel}{L_{\parallel 0}}=\frac{b}{\gamma}, \qquad \frac{L_\perp}{L_{\perp 0}}=b \tag{8}$$

Continuous equality of clock rates and restoration of the reference longitudinal length therefore require $b=\gamma$. The transverse dimensions retain the factor b. Equal rates preserve equal readings when the clocks begin synchronized; an earlier accumulated offset remains a separate quantity. In the OQG material interpretation, loaded contraction names the longitudinal Lorentz response already represented in Eq. (8). Mechanical strain from a support or engine is an additional material disturbance with its own response calculation.

For one-dimensional motion, take u to be signed along the chosen axis. The matched scale and velocity must solve Eq. (7) together because c_b also changes. Their relation is

$$b=\gamma\geq 1, \qquad \frac{u^2}{c_b^2}=1-b^{-2}, \qquad u_{\pm}=\pm c_0 b\sqrt{b^2-1} \tag{9}$$

Each finite member remains below its applicable propagation speed c_b. Equation (9) supplies the velocity setpoint associated with a prepared scale. The propulsion and controller equations determine how that setpoint is reached and maintained. Matching these comparisons by itself specifies neither an accelerometer reading nor a reduction in passenger loads.

Let V_0 be the original volume and $\overline{\varepsilon}_0=E_0/V_0>0$ its average rest-state energy density. Let V_b and $\overline{\varepsilon}_b$ denote the prepared values, and define the density contrast $\Delta\overline{\varepsilon}=\overline{\varepsilon}_b-\overline{\varepsilon}_0$. The required changes are

$$\begin{gathered} V_b=b^3V_0, \qquad \overline{\varepsilon}_b=b^{-2}\overline{\varepsilon}_0 \\ \left.\frac{\overline{\varepsilon}_b}{\overline{\varepsilon}_0}\right|_{b=\gamma}=\gamma^{-2} \\ \Delta\overline{\varepsilon}=\overline{\varepsilon}_0(b^{-2}-1)<0 \quad \text{for } b>1 \end{gathered} \tag{10}$$

The density reduction is a necessary material requirement of this matched family. The same body contains more rest energy, occupies a still larger volume, and has a lower positive density. Its negative contrast with the reference is not a negative total energy or an identified exotic warp source. Section V shows where the added work resides and how the density labels that stored energy. Any energy-condition assessment separately requires the complete stress tensor of the body, source, and boundaries.

The accumulated clock difference will be needed for the terrestrial example. Let t_i be the initial event and $\delta\tau(t)$ the spacecraft reading minus the reference reading, with ϑ a time integration variable. Then

$$\delta\tau(t)=\delta\tau(t_i)+\int_{t_i}^{t}\left[\frac{b(\vartheta)}{\gamma(\vartheta)}-1\right]\mathrm{d}\vartheta \tag{11}$$

This integral records departures during any interval when rate matching is interrupted. The flight in Section VIII uses matched powered segments and an explicitly calculated ballistic turnaround. The result of the material comparison is now definite: continuous compensation requires $b=\gamma$, increased rest energy, and a positive density reduced by γ^{-2}. The controller must produce all of these changes in the same bound matter. The quantum construction next explains what that preparation means internally.

IV. Matter waves specify the coordinated quantum preparation

The generator must enlarge the bound matter itself while raising its transition energies. Changing one measured frequency or stretching the hull would leave the rest of that requirement unresolved. The spatial pattern and binding of the quantum state must change together. The following construction identifies that coordinated preparation and explains why a larger body can have smaller internal momentum intervals yet greater rest energy.

Begin with an internal coordinate x, distinct from the spacecraft trajectory. Let p be its canonical momentum, k the spatial wave number, λ the wavelength, and $\hbar$ the fixed reduced Planck constant. Canonical momentum is the momentum paired with position in the quantum description. A Fourier component has phase $px/\hbar=kx$; one spatial cycle gives the de Broglie relations [14]

$$p=\hbar k, \qquad \lambda=\frac{2\pi}{|k|}=\frac{2\pi\hbar}{|p|}, \qquad |p|\lambda=2\pi\hbar \tag{12}$$

These expressions use a nonzero component. With an applied vector potential, canonical and mechanical momentum can differ; the potential contribution then enters the physical phase comparison. The observable preparation must remain independent of the choice of gauge, meaning the potential representation used for the same physical field.

Two coherent components with momenta p_1 and p_2 have a well-defined relative phase. Define their nonzero momentum gap by $\delta p_{12}=p_2-p_1$ and their interference interval by ℓ_{12}. Similarly, let $\Delta E_{\mathrm{tr}}>0$ be a clock transition gap and T_{cl} its period. The spatial and temporal relative phases give

$$\ell_{12}=\frac{2\pi\hbar}{|\delta p_{12}|}, \qquad T_{\mathrm{cl}}=\frac{2\pi\hbar}{\Delta E_{\mathrm{tr}}} \tag{13}$$

A smaller momentum gap produces a larger spatial interval; a larger energy gap produces a shorter clock period. Neither gap is a statistical variance. A wavelength, an interference interval, and the overall extent of a localized state are also different lengths. An ideal plane wave has a definite wavelength and extends throughout space. A localized packet combines momentum components whose amplitudes and relative phases form an envelope. Changing its central momentum can change the carrier wavelength while leaving the envelope's size unchanged. Enlarging bound matter requires the complete corresponding pattern and its binding to scale together [15].

A standing mode makes the distinction visible. In a one-dimensional ideal well of length L, a positive integer mode label n gives $k_n=n\pi/L$ and counterpropagating momenta $\pm\hbar k_n$. Their mean momentum can vanish even though both components are nonzero. The wave has wavelength $2L/n$, while its probability-density pattern repeats

over L/n. Increasing the well and the corresponding mode by b enlarges both intervals and reduces both momenta by b^{-1}. Raising the energy at the same time requires the transformed binding Hamiltonian derived below.

Let X and P be the internal position and conjugate momentum operators, with commutator $[X,P]=XP-PX=i\hbar I$. Here i is the imaginary unit and I the identity. Define the dilation generator D and unitary transformation U_b below. A dagger denotes the adjoint. On a common domain where these operators and products are defined [16],

$$D=\frac{1}{2}(XP+PX), \qquad U_b=\exp\left(-\frac{i\ln b}{\hbar}D\right)$$
$$U_b^\dagger X U_b=bX, \qquad U_b^\dagger P U_b=b^{-1}P \tag{14}$$

The commutators $[D,X]=-i\hbar X$ and $[D,P]=i\hbar P$ give the reciprocal factors. Three-dimensional scaling uses the sum over the three coordinate generators. Let $\psi_0(\mathbf{x})$ be a normalized wavefunction for one internal three-dimensional coordinate and $\tilde{\psi}_0(\mathbf{p})$ its Fourier momentum amplitude. Bold symbols denote vectors. The transformed amplitudes are

$$\psi_b(\mathbf{x})=b^{-3/2}\psi_0(\mathbf{x}/b)$$
$$\tilde{\psi}_b(\mathbf{p})=\frac{1}{(2\pi\hbar)^{3/2}}\int \mathrm{d}^3x\, e^{-i\mathbf{p}\cdot\mathbf{x}/\hbar}\psi_b(\mathbf{x})=b^{3/2}\tilde{\psi}_0(b\mathbf{p}) \tag{15}$$

The normalization factors preserve total probability. Substitution of $\mathbf{x}=b\mathbf{y}$, with $\mathbf{y}$ a rescaled integration coordinate, gives the second line. Corresponding features of the full spatial pattern enlarge while the momentum components move closer together. Their relative amplitudes and phases remain those of the corresponding state. With L_b a characteristic bound-state extent,

$$p_b=b^{-1}p_0, \qquad \delta p_{12,b}=b^{-1}\delta p_{12,0}$$
$$\lambda_b=b\lambda_0, \qquad \ell_{12,b}=b\ell_{12,0}, \qquad L_b=bL_0 \tag{16}$$

For a statistical mixture, let ρ_0 be the normalized density operator and $\rho_b=U_b\rho_0U_b^\dagger$ the transformed state. With tr denoting the trace, $\mathrm{tr}(\rho O)$ is the mean of an observable O. Let $\mathcal{P}_b$ denote position probability density. Define ΔX and ΔP as standard deviations, whose squares are variances. Then

$$\mathcal{P}_b(\mathbf{x})=b^{-3}\mathcal{P}_0(\mathbf{x}/b), \qquad \Delta X_b=b\Delta X_0, \qquad \Delta P_b=b^{-1}\Delta P_0 \tag{17}$$

The uncertainty product $\Delta X\Delta P\geq\hbar/2$ retains its value. The exact factors follow from the specified dilation; the inequality supplies its consistency bound. Correlations give an additional check. Write $\langle X\rangle$ for a mean, define $\delta X=X-\langle X\rangle$ and $\delta P=P-\langle P\rangle$, and let $C_{XP}=\langle\{\delta X,\delta P\}\rangle/2$. The braces denote the anticommutator, $\{A,B\}=AB+BA$. Let

diag denote a diagonal matrix, superscript T a transpose, and det a determinant. The covariance matrix Σ and scaling matrix S_b obey

$$\Sigma=\begin{pmatrix}(\Delta X)^2 & C_{XP}\\ C_{XP} & (\Delta P)^2\end{pmatrix}, \qquad \det\Sigma\geq\frac{\hbar^2}{4}$$
$$S_b=\mathrm{diag}(b,b^{-1}), \qquad \Sigma_b=S_b\Sigma_0S_b^{\mathrm{T}}, \qquad \det\Sigma_b=\det\Sigma_0 \tag{18}$$

The transformed state preserves the covariance determinant whether or not it saturates the quantum bound.

Let H_0 be the reference Hamiltonian, and let $|n\rangle$ denote an energy eigenstate with eigenvalue E_n, so that $H_0|n\rangle=E_n|n\rangle$. The binding Hamiltonian required to realize the common length and energy scaling of Eq. (6) is

$$H_b=bU_bH_0U_b^{\dagger}, \qquad |n;b\rangle=U_b|n\rangle$$
$$H_b|n;b\rangle=bE_n|n;b\rangle \tag{19}$$

The conjugation changes the spatial binding problem, and the leading factor b raises its corresponding energies. If the reference state is stationary, $[H_0,\rho_0]=0$, then $[H_b,\rho_b]=0$. Its level populations remain fixed, and its mean energy becomes $\mathrm{tr}(\rho_bH_b)=b\mathrm{tr}(\rho_0H_0)$. A smaller internal momentum scale can therefore coexist with higher energy because the kinetic coefficients and binding have changed together. Dilation alone fixes the reciprocal position and momentum factors; the prefactor b implements the stipulated common energy scaling.

For a clock transition, the angular frequency is $\omega=\Delta E_{\mathrm{tr}}/\hbar$. Equation (19) gives

$$\Delta E_{\mathrm{tr},b}=b\Delta E_{\mathrm{tr},0}, \qquad \omega_b=b\omega_0, \qquad T_{\mathrm{cl},b}=b^{-1}T_{\mathrm{cl},0} \tag{20}$$

At rest relative to the reference, the prepared clock completes more cycles per unit retained reference time. Thus the same quantum family supplies both the enlarged ruler and the faster clock in Section III. The clock period follows the relative phase of energy levels; this construction requires no universal time operator. With $\mathrm{d}\ln b=\mathrm{d}b/b$ denoting a fractional change, its reciprocal control relations are

$$\mathrm{d}\ln\lambda=-\mathrm{d}\ln|p|=\mathrm{d}\ln b$$
$$\mathrm{d}\ln\ell_{12}=-\mathrm{d}\ln|\delta p_{12}|=\mathrm{d}\ln b$$
$$\mathrm{d}\ln T_{\mathrm{cl}}=-\mathrm{d}\ln\Delta E_{\mathrm{tr}}=-\mathrm{d}\ln b \tag{21}$$

The corresponding nonzero modes and gaps are followed throughout. In a geometric description, measured intervals organize these energy and momentum comparisons. In OQG's engineering description, source interactions prepare the spectrum and binding, and the material intervals are their outputs. GR's coupled matter and field equations retain their usual mutual dependence; the distinction concerns the physical system taken as primary.

The required inflation is therefore a change of the whole bound quantum state. Its longer spatial pattern and faster transitions arise together because both the state and its Hamiltonian change. The canonical dilation preserves its quantum consistency. The increased energy is carried by this prepared matter, which makes the location and amount of the lifting work the next physical question.

V. Gravitational potential energy is stored in the changed bound state

Lift an object from the floor to a shelf and leave it at rest. Work has been done, and lowering the object can return that energy. In OQG's common-scale description, this work is stored as the increase in the body's bound material-state energy relative to the floor reference. That increase is its assigned gravitational potential energy. The object has a slightly larger equilibrium structure and higher corresponding internal energies. Its energy density falls because its volume increases faster than its total energy. This storage mechanism gives the preparation a physical energy account.

Take a small object in Earth's slowly varying ambient, and retain the floor clock and energy standards as reference state 0. Set the scale there to b=1. Compare settled states with the same material content and level populations, treating heating, support strain, and losses separately. Let E_0=tr($\rho_0 H_0$) be the complete reference body energy, including its binding fields and stresses. For two scales b_1 and b_2, Section IV gives

$$E_{\text{body}}(b)=\text{tr}(\rho_b H_b)=bE_0, \qquad \Delta E_{\text{body}}=E_0(b_2-b_1) \tag{22}$$

The work is carried by the constituent fields, internal motion, and binding correlations of the changed body state, expressed in the retained external standards. Equation (19) specifies how it is stored: the Hamiltonian's energy scale rises and its binding structure expands, while corresponding level populations remain fixed. The body therefore occupies a different equilibrium state rather than simply receiving a heat load. Its rest energy grows with b, while its equilibrium volume grows with b^3.

The energy distribution makes that distinction explicit. Let $\varepsilon_0(\mathbf{x})$ be the reference distribution averaged over microscopic detail, and let $\mathscr{B}_0$ contain the complete body. In the self-similar limit the prepared domain is $\mathscr{B}_b=b\mathscr{B}_0$. With $\mathbf{y}=\mathbf{x}/b$,

$$\varepsilon_b(\mathbf{x})=b^{-2}\varepsilon_0(\mathbf{x}/b)$$
$$\int_{\mathscr{B}_b}\varepsilon_b(\mathbf{x})\,\mathrm{d}^3x=b\int_{\mathscr{B}_0}\varepsilon_0(\mathbf{y})\,\mathrm{d}^3y=bE_0 \tag{23}$$

The expanded integration domain is essential. Each corresponding volume element carries lower energy density, but the complete volume is larger by a greater factor. Their product gives the increased energy bE_0. Comparing densities only within the original volume would miss part of the prepared body. Binding fields extending beyond the material surface belong in the complete-body boundary. Equation (23) states the self-similar limit; the full response determines departures from it.

Let U_{grav} be the gravitational potential-energy increase assigned to the body relative to b_1, and let $W_{\mathrm{lift,rev}}$ denote ideal reversible lifting work. The OQG identification is

$$W_{\mathrm{lift,rev}}=U_{\mathrm{grav}}(b;b_1)=\Delta E_{\mathrm{body}}=E_0(b-b_1) \tag{24}$$

Equation (24) identifies the storage directly: the lifting work and the body's increase in bound-state energy are the same contribution. Adding a separate copy of gravitational potential energy would count that work twice. The assignment remains relational. Earth establishes the ambient and the floor fixes the comparison; Earth, the lifting apparatus, interaction boundaries, and losses complete the system account, with each contribution counted once.

With b_1=1, the average density can label the prepared state. Eliminating b using Eq. (10) gives

$$U_{\mathrm{grav}}=E_0\left(\sqrt{\frac{\bar{\varepsilon}_0}{\bar{\varepsilon}_b}}-1\right)$$
$$\frac{\mathrm{d}E_b}{E_b}=\mathrm{d}\ln b, \qquad \frac{\mathrm{d}\bar{\varepsilon}_b}{\bar{\varepsilon}_b}=-2\,\mathrm{d}\ln b \tag{25}$$

Equation (25) makes the density relation usable as an energy label: lower positive density corresponds to greater stored lifting energy within this family. Returning toward the floor reduces that rest-state contribution, which can become motion or recovered work.

To recover the ordinary lifting result, let Φ be Newtonian potential per unit mass and Φ_0 its floor value. Define reference mass $M_0=E_0/c_0^2$, and let ∇ denote the spatial gradient. In a weak static field, $b-1\simeq(\Phi-\Phi_0)/c_0^2$. The work and its conjugate force $\mathbf{F}_{\mathrm{grav}}$ are then

$$U_{\mathrm{grav}}\simeq M_0(\Phi-\Phi_0), \qquad \mathbf{F}_{\mathrm{grav}}=-E_0\nabla b\simeq -M_0\nabla\Phi \tag{26}$$

For a height increase z in nearly constant gravity g, the work is M_0gz. The force points toward lower potential and lower scale. This reference-work definition fixes the sign and recovers the familiar result before the same body-state account is applied to controlled spacecraft preparation.

The static GR comparison provides the same reference-energy difference. Let N be the clock-rate factor of a local static observer relative to the chosen reference, and let E_{loc} be the body's energy measured by that observer. Time-translation symmetry defines conserved Killing energy E_ξ [9]. For corresponding static states at fixed E_{loc},

$$E_\xi = N E_{\mathrm{loc}}, \qquad \Delta E_\xi = E_{\mathrm{loc}}(N_2 - N_1) \tag{27}$$

Identifying $N=b$ gives Eq. (24). OQG interprets that comparison through the corresponding material state. Co-scaling instruments retain their dimensionless readings, including a local calorimeter's reading relative to its own standards. The body-state assignment is made under these declared conditions; energies for the entire gravitational system require the appropriate global or finite-boundary construction [10].

For propelled compensation, distinguish this rest-state work from kinetic energy. Let $E_{\mathrm{mov}}=\gamma b E_0$ be the assigned moving energy, $K=E_{\mathrm{mov}}-E_b$ its kinetic contribution, and $W_{\mathrm{body}}=E_{\mathrm{mov}}-E_0$ the total receiving-body increase. Along $b=\gamma$,

$$\Delta E_{\mathrm{rest}} = E_0(b-1), \qquad K = E_0 b(b-1)$$
$$W_{\mathrm{body}} = E_0(b^2-1) \tag{28}$$

The fixed material content here excludes separately consumed source resources and propellant. In the weak-scale, low-speed limit of Eq. (9),

$$b-1 \simeq \frac{u^2}{2c_0^2}, \qquad \Delta E_{\mathrm{rest}} \simeq \frac{1}{2} M_0 u^2, \qquad W_{\mathrm{body}} \simeq M_0 u^2 \tag{29}$$

The preparation contribution equals the leading ordinary kinetic-energy increment for the same reference mass and speed. Their sum is twice that ordinary increment. This gives the compensation an explicit positive work requirement as speed increases. A controller and a rocket can supply different parts of that work, so the force allocation requires their actual coupling. Section IX develops the time-dependent power and spatial response needed to make that allocation.

The density reduction is part of the energy-storage requirement. A practical source must prepare the higher-energy, larger bound state across electronic and nuclear structure while its propulsion reaction remains accounted for.

VI. Electronic and nuclear binding follow the same material scale

The generator must prepare the matter that holds the spacecraft together. Atomic dimensions, clock transitions, nuclear rest energy, and mechanical integrity must follow the same corresponding-state change. Electronic and nuclear binding therefore test whether the proposed expansion describes a complete material state. Their forces, spectra, and equilibrium fluctuations specify what the enlarged matter must retain.

Let $\mathcal{V}_0(\mathbf{x})$ be a binding potential for a resolved internal coordinate, and let $\mathbf{F}_0=-\nabla\mathcal{V}_0$ be its force. The Hamiltonian family in Eq. (19) requires

$$\mathcal{V}_b(\mathbf{x})=b\mathcal{V}_0(\mathbf{x}/b), \qquad \mathbf{F}_b(b\mathbf{x}_0)=\mathbf{F}_0(\mathbf{x}_0) \tag{30}$$

At corresponding separation, the increase in energy scale cancels the increase in distance when the slope is taken. The potential curvature instead scales by b^{-1}, so the restoring stiffness per unit reference displacement changes. The equilibrium force and stiffness describe different properties of the preparation.

For an explicit check, let m_0 and ω_0 be the reference mass coefficient and angular frequency of one harmonic mode. Applying the same transformation to its kinetic and potential energies gives

$$H_b=\frac{b^3P^2}{2m_0}+\frac{m_0\omega_0^2X^2}{2b}, \qquad m_b=b^{-3}m_0, \qquad \omega_b=b\omega_0 \tag{31}$$

Both the inertia coefficient and restoring coefficient change, and together they increase the frequency by b. The coefficient m_b agrees with E_b/c_b^2 on the common-scale family. This is an internal-mode consistency check; the complete spacecraft response still includes its interacting constituents and supports.

Electronic structure sets atomic dimensions and many clock transitions. Quantum chromodynamics (QCD), the strong-interaction theory of quarks and gluons, underlies the nucleons and their nuclear binding. Let E_e denote electron rest energy, α the fine-structure constant, and Λ_{QCD} a characteristic strong-interaction energy. Let ζ collect dimensionless composition and coupling data, and $f_{\mathrm{N}}(\zeta)$ describe the selected nucleus. With c the propagation speed in the compared state, the reduced Compton wavelength $\overline{\lambda}_e$, Bohr length a_{B}, and nuclear radius R_{N} have representative forms

$$\overline{\lambda}_e=\frac{\hbar c}{E_e}, \qquad a_{\mathrm{B}}=\frac{\hbar c}{\alpha E_e}, \qquad R_{\mathrm{N}}=\frac{\hbar c}{\Lambda_{\mathrm{QCD}}}f_{\mathrm{N}}(\zeta) \tag{32}$$

The atomic expression uses the leading hydrogenic scale; the reduced-mass correction has a fixed dimensionless ratio in corresponding states. Each length grows by b when its characteristic energy grows by b, c grows by b^2, and

its dimensionless data remain fixed. Nuclear stability additionally requires the interacting spectrum and allowed decay channels to remain compatible with that family.

Conserved charge gives another check. Let Q be the charge operator. If the chosen dilation commutes with charge, its mean is preserved:

$$[U_b,Q]=0 \quad \Rightarrow \quad \mathrm{tr}(\rho_b Q)=\mathrm{tr}(\rho_0 Q) \tag{33}$$

At fixed α and $\hbar$, the Coulomb force proportional to $\alpha\hbar c/r^2$ also remains unchanged at corresponding separation $r_b=br_0$. This reproduces Eq. (30) while retaining the charge content.

Most of ordinary matter's rest energy resides in nuclei, so their quantum degrees of freedom are part of the controller target. Gluons are bosons and quarks are fermions; their exchange rules give commutators and anticommutators, respectively [17, 18]. Let $A_i^a(\mathbf{x},t)$ denote a gluon potential and $\Pi_j^c(\mathbf{y},t)$ its canonical momentum. The indices i,j label spatial components, and a,c label color, the strong-interaction charge components. Discrete deltas equal one when their indices match and zero otherwise; $\delta^{(3)}$ is the three-dimensional Dirac delta. In temporal gauge, which sets the time component of the potential to zero, the auxiliary field description has the equal-time relation

$$\left[A_i^a(\mathbf{x},t),\Pi_j^c(\mathbf{y},t)\right]=i\hbar\delta_{ij}\delta^{ac}\delta^{(3)}(\mathbf{x}-\mathbf{y}) \tag{34}$$

Gauss's law then selects physical states from this auxiliary space. For a quark field ψ_α^a, let α,β label spinor components; these indices are distinct from the scalar fine-structure constant. For the same quark flavor on both sides, the usual normalization gives

$$\{\psi_\alpha^a(\mathbf{x},t),\psi_\beta^{c\dagger}(\mathbf{y},t)\}=\delta^{ac}\delta_{\alpha\beta}\delta^{(3)}(\mathbf{x}-\mathbf{y}) \tag{35}$$

The equivalent field–momentum relation uses $\pi_\psi=i\hbar\psi^\dagger$ and retains $i\hbar$ on its right side. The absence of an explicit $\hbar$ in Eq. (35) follows from field normalization. Physical controller outputs are bound-state properties and the completed stress response after the gauge constraints are imposed.

The harmonic mode makes the elementary zero-point content explicit. For integer n=0,1,…, its reference spectrum and ground-state variances are

$$E_n=\hbar\omega_0\left(n+\frac{1}{2}\right), \qquad (\Delta X_0)^2=\frac{\hbar}{2m_0\omega_0}, \qquad (\Delta P_0)^2=\frac{\hbar m_0\omega_0}{2} \tag{36}$$

The ground energy is $\hbar\omega_0/2$ relative to the potential minimum; $\hbar/2$ is an action scale. Under the preparation, the energy increases by b and the two variances acquire the reciprocal factors in Section IV. Thus a larger spatial distribution is consistent with greater ground-state energy when binding and inertia change together.

Interacting nuclear matter combines fermionic exchange, gluon self-interaction, confinement, and correlations. Quarks and gluons form hadrons, including protons and neutrons, while residual interactions bind those nucleons into nuclei. A stable ground state has no lower allowed state into which it can radiate while respecting the conservation laws. Its quantum fluctuations and binding belong to that equilibrium description.

Mechanical equilibrium provides a direct stress check. For a static, localized, spherically symmetric hadronic state, let $r=|\mathbf{r}|$ be radius, $p_{\text{press}}(r)$ pressure, $s(r)$ shear stress, and T^{ij} the complete spatial stress. Stress conservation gives the decomposition and necessary integrated balance [19]

$$T^{ij}(\mathbf{r})=\left(\frac{r^i r^j}{r^2}-\frac{\delta^{ij}}{3}\right)s(r)+\delta^{ij}p_{\text{press}}(r)$$
$$\partial_i T^{ij}=0, \qquad \int_0^\infty r^2\, p_{\text{press}}(r)\,\mathrm{d}r=0 \tag{37}$$

The pressure integral balances inward and outward contributions. Binding energies, radii, and nuclear saturation provide further stability tests and depend on the appropriate two-nucleon, three-nucleon, and other interactions [20]. QCD also has scale-dependent couplings and a trace anomaly, the quantum contribution that introduces a physical scale into the stress trace. The required change in Λ_{QCD} expressed in external standards must follow from that interacting response.

Equilibrium fluctuations and damping are linked parts of the same physical account. Electromagnetic equilibrium models provide useful motivation [21, 22], and the quantum Langevin description retains fluctuating forces consistently with dissipation [23]. For the coordinate X, let a weak force $f(t)$ couple through energy $-f(t)X$. Define the retarded susceptibility by $\chi^R_{XX}(t)=(i/\hbar)\theta(t)\langle[X(t),X(0)]\rangle$, where $\theta(t)$ is the step function, and use Fourier convention $F(\omega)=\int\mathrm{d}t\, e^{i\omega t}F(t)$. Superscript R denotes the retarded response, which vanishes before the disturbance.

Let $S_{XX}(\omega)$ be the symmetrized fluctuation spectrum, k_{B} Boltzmann's constant, and T_{th} temperature. With Im the imaginary part and coth the hyperbolic cotangent, the equilibrium fluctuation–dissipation relation for the relaxing degrees of freedom is [24]

$$\begin{gathered} S_{XX}(\omega)=\int_{-\infty}^{\infty}\mathrm{d}\,t\,e^{i\omega t}\,\frac{1}{2}\langle\{\delta X(t),\delta X(0)\}\rangle \\ S_{XX}(\omega)=\hbar\coth\left(\frac{\hbar\omega}{2k_{\mathrm{B}}T_{\mathrm{th}}}\right)\mathrm{Im}\chi_{XX}^{R}(\omega) \\ (\Delta X)^2=\int_{-\infty}^{\infty}\frac{\mathrm{d}\omega}{2\pi}S_{XX}(\omega) \end{gathered} \tag{38}$$

The dissipative response and equilibrium noise must therefore describe the same state. For a Hermitian stress observable O, with real measurement outcomes and a finite spatial averaging region, define its connected spectrum and susceptibility in the same way. Static conserved contributions are treated separately. At zero temperature and nonzero frequency, with sgn denoting the sign function,

$$S_{OO}(\omega)=\hbar\mathrm{sgn}(\omega)\mathrm{Im}\chi_{OO}^{R}(\omega) \tag{39}$$

The stress observable obeys this bosonic response relation even when its constituents include fermions. Its spectrum describes allowed disturbances and the fluctuations of the settled state.

For corresponding thermal states, fixed level populations require $T_{\mathrm{th},b}=bT_{\mathrm{th},0}$ in external units. The dilation multiplies displacement by b, and the Hamiltonian multiplies the evolution's time argument by b. The coordinate response and spectrum consequently transform as

$$\begin{gathered} \chi_{XX,b}^{R}(\omega)=b\chi_{XX,0}^{R}(\omega/b),\qquad S_{XX,b}(\omega)=bS_{XX,0}(\omega/b) \\ (\Delta X_b)^2=b^2(\Delta X_0)^2 \end{gathered} \tag{40}$$

The spectrum changes in amplitude and frequency, yielding the required variance on integration. Electronic, nuclear, and macroscopic binding consequently impose one linked requirement on the generator: enlarge the equilibrium structure, raise its energy scale, and preserve a stable interacting state. A clock shift alone establishes only one part of that requirement. The causal stress response must connect these settled states to an interaction that can actually prepare them.

VII. The complete stress response determines the material control target

The material scale must be connected to a response that a physical source can produce. The same interacting matter that stores the lifting work carries energy, momentum, pressure, and shear. Its completed response fixes the

settled coefficient used to compare states. The normalization below shows how that coefficient enters the adopted gravitational representation and identifies the additional inputs needed to make the connection explicit.

OQG evaluates that response using the closed-time-path construction [25, 26]. Two mathematical source histories are evolved forward and backward, differentiated independently, and then compared. This construction computes the causal effect of disturbances in an interacting quantum state. Let q_B denote a symmetric tensor probe coupled to complete stress T_A, where capital indices combine tensor components and spacetime arguments. Define the susceptibility Π^R_{AB} as the variation of mean stress under the probe, and $\mathcal{D}^R$ as its inverse on the independent physical response components:

$$\Pi^R_{AB}=\frac{\delta\langle T_A\rangle}{\delta q_B}=\Pi^{R,\mathrm{conn}}_{AB}+\Pi^{R,\mathrm{contact}}_{AB}$$
$$\mathcal{D}^R=\left(\Pi^R_{\mathrm{phys}}\right)^{-1} \tag{41}$$

The connected contribution contains stress correlations with products of separate means removed. The contact contribution comes from the explicit variation of the stress operator. Conservation identities apply to their complete sum [2, 3]. The physical projection selects independent response directions before the retarded inverse is taken. Products include integrations over intermediate spacetime points. An actual controller supplies a history through its matter and interactions; the probe is the mathematical means of calculating that response.

The settled common-scale relation uses the total spectral stiffness $A^{\mathrm{tot}}_{2,\mathrm{E}}$. It is the coefficient of the two-derivative static shear response after the transverse-traceless projection, which selects shear perpendicular to the disturbance wave vector and removes the trace. The label E denotes Euclidean evaluation, the mathematical continuation used for this static coefficient. Its units are energy squared; it is distinct from the restoring stiffness per unit displacement in Section VI, which scales inversely with the material scale. Let ρ_{ref} be a declared reference preparation and $A_{2,\mathrm{E}}[\rho;\rho_{\mathrm{ref}}]$ the calculated state difference. The total coefficient is

$$A^{\mathrm{tot}}_{2,\mathrm{E}}[\rho]=A^{\mathrm{tot}}_{2,\mathrm{E}}[\rho_{\mathrm{ref}}]+A_{2,\mathrm{E}}[\rho;\rho_{\mathrm{ref}}] \tag{42}$$

The reference term fixes the intercept needed to compare total coefficients in the declared standards. A high-temperature Standard-Model calculation supplies a state difference. Its specified inputs include the Higgs improvement coupling, which fixes a curvature coupling of the Higgs field, and finite magnetic response constants for the strong and weak sectors [27, Secs. 2–4]. Cold bound matter and a spacecraft source require the susceptibility of their own prepared states. The reference contribution remains necessary in either case.

The normalization starts with a definite microscopic coefficient. Let k be a spatial wave number in inverse-length units and $Q=\hbar ck$ its energy-unit counterpart. Let $\Delta G_{\mathrm{E}}(Q)$ be the completed Euclidean shear correlator of the prepared state minus that of its reference, including the contact contribution. Define $\Delta\kappa$ as its second derivative at $Q=0$. The symmetric-source convention of Ref. [2, Sec. 2, Eqs. (3)–(4)] gives

$$\Delta G_{\mathrm{E}}(Q)=\Delta G_{\mathrm{E}}(0)+\frac{\Delta\kappa}{2}Q^2+O(Q^4)$$
$$A_{2,\mathrm{E}}[\rho;\rho_{\mathrm{ref}}]=\frac{\Delta\kappa}{4} \tag{43}$$

Here $O(Q^4)$ denotes terms beginning at fourth order in the small-wave-number expansion. Let ${G_E}^{12,12}(0,Q)$ be the completed shear correlator before taking a preparation difference. In the symmetric-source convention of Ref. [2], its TT polarization is $\Pi_{\mathrm{TT,E}}$. Remove the zero-wave-number equilibrium preload and retain the positive derivative block on the selected stable branch. This defines the static constitutive kernel $\mathcal{K}_{\mathrm{TT,E}}$ and its inverse $\mathcal{D}_{\mathrm{TT,E}}$:

$$\Pi_{\mathrm{TT,E}}(Q)=-\frac{1}{2}{G_E}^{12,12}(0,Q)$$
$$\mathcal{K}_{\mathrm{TT,E}}(Q)=-[\Pi_{\mathrm{TT,E}}(Q)-\Pi_{\mathrm{TT,E}}(0)]=A_{2,\mathrm{E}}^{\mathrm{tot}}Q^2+O(Q^4)$$
$$\mathcal{D}_{\mathrm{TT,E}}(Q)=\mathcal{K}_{\mathrm{TT,E}}^{-1}(Q)=\frac{1}{A_{2,\mathrm{E}}^{\mathrm{tot}}Q^2}+O(Q^0) \tag{44}$$

Equation (41) inverts the full completed physical susceptibility. Equation (44) instead inverts its static TT derivative block after the stated source normalization, sign choice, and preload subtraction. Projection and subtraction precede this second inversion; the two inverses are distinct. The latter has inverse-distance leading spatial behavior and supplies the gravitational matching. A signed coefficient in the equilibrium matter functional is a different object [2, Secs. 2–3].

The Einstein-equivalent representation uses a selected causal branch with massless tensor disturbances of two helicities, the two independent polarization states. A fixed-measure completion with transverse diffeomorphisms and Weyl redundancy, abbreviated WTDiff, supplies the nonlinear representation [2, 28, 29]. Transverse transformations preserve the integration measure, and Weyl redundancy is a local rescaling freedom of the auxiliary tensor. WTDiff provides the economical fixed-measure completion adopted here. The static two-point coefficient alone leaves this choice open; the completion is an additional assumption, not a uniquely derived consequence of that coefficient.

Once that choice is stated, its normalization can be checked directly. In one fixed state, use inverse-energy coordinates $\Xi^\mu=x^\mu/(\hbar c)$, where $x^0=ct$ and Greek indices label the four spacetime components. Let $V_4=\int \mathrm{d}^4\Xi$ be the regulated four-volume and use a real dimensionless shear $h_{12}=h_{21}=h_Q e^{iQ\Xi^3}+h_{-Q}e^{-iQ\Xi^3}$, with $h_{-Q}=h_Q^*$ and the

asterisk denoting complex conjugation. Let $\Gamma^{(2)}_{\mathrm{TT,E}}$ and $\Gamma^{(2)}_{\mathrm{W,E}}$ be the dimensionless quadratic tensor-response and WTDiff actions for that same shear. Define C_{W} as the WTDiff curvature-action coefficient in these coordinates. Counting both symmetric components and both Fourier amplitudes gives [2, Sec. 4, Eqs. (18)–(20)]

$$\Gamma^{(2)}_{\mathrm{TT,E}}=2A^{\mathrm{tot}}_{2,\mathrm{E}}V_4Q^2h_Qh_{-Q}$$
$$\Gamma^{(2)}_{\mathrm{W,E}}=C_{\mathrm{W}}V_4Q^2h_Qh_{-Q}, \qquad C_{\mathrm{W}}=2A^{\mathrm{tot}}_{2,\mathrm{E}} \tag{45}$$

The factor of two follows from the common source convention. To restore physical units, let G denote the gravitational coupling, ϖ the fixed integration density, R the curvature scalar formed with length coordinates, and $R_{\mathrm{en}}=(\hbar c)^2R$ its energy-coordinate counterpart. The Einstein-normalized action S_{W} is [2, Sec. 5, Eqs. (24)–(26)]

$$\frac{S_{\mathrm{W}}}{\hbar}=\frac{c^3}{16\pi\hbar G}\int \mathrm{d}^4x\,\varpi R$$
$$=\frac{\hbar c^5}{16\pi G}\int \mathrm{d}^4\Xi\,\varpi R_{\mathrm{en}}, \qquad C_{\mathrm{W}}=\frac{\hbar c^5}{16\pi G} \tag{46}$$

These coordinate conversions compare coefficients within one state. Comparison between different prepared states retains the changing c explicitly and keeps $\hbar$ fixed. Combining Eqs. (45) and (46) supplies the adopted normalization. On the stated common-scale branch,

$$A^{\mathrm{tot}}_{2,\mathrm{E}}=\frac{\hbar c^5}{32\pi G}, \qquad b=\left(\frac{A^{\mathrm{tot}}_{2,\mathrm{E}}[\rho_b]}{A^{\mathrm{tot}}_{2,\mathrm{E}}[\rho_0]}\right)^{1/2}$$
$$\frac{G_b}{c_b^4}=\frac{G_0}{c_0^4}, \qquad c_b=b^2c_0, \qquad G_b=b^8G_0 \tag{47}$$

The invariant force coupling is G/c^4, while $\hbar$ remains fixed and the external propagation comparison changes with the prepared state. The completed total spectral stiffness determines the common-scale label under the stated branch conditions [1, 16]. The trace-free variation and integrated Einstein-equivalent equations of the selected completion are given in Ref. [2, Sec. 6, Eqs. (33)–(37)]. Its causal bandwidth, dissipation, and relaxation remain properties of the full response in Eq. (41).

To connect the coefficient to material standards, let E_c be a common characteristic energy. At fixed dimensionless data ζ, define the dimensionless functions $a_2(\zeta)$, $f_a(\zeta)$, and $\ell_a(\zeta)$ for the response, clock transition, and ruler construction. Then

$$A^{\mathrm{tot}}_{2,\mathrm{E}}=E_c^2a_2(\zeta), \qquad \omega_a=\frac{E_c}{\hbar}f_a(\zeta), \qquad L_a=\frac{\hbar c}{E_c}\ell_a(\zeta) \tag{48}$$

At fixed ζ, the spectral-stiffness ratio gives $E_c/E_{c0}=b$. Together with $c_b/c_0=b^2$, this reproduces the frequency and length factors in Section III. For matched operation the required total spectral-stiffness ratio is therefore γ^2, while the rest-state density ratio is γ^{-2}.

The normalization now connects a defined microscopic shear coefficient to the adopted gravitational coupling, with the source factors, reference contribution, and completion choice visible. Together with the corresponding-state relations, it demands a spectral-stiffness increase of γ^2 and a positive density decrease of γ^{-2} for matched operation. These are physical outputs to be established throughout the receiving matter. Earth supplies a natural ambient in which their trajectory and energy consequences can be calculated before an artificial generator is proposed.

VIII. A terrestrial flight experiment tests matched clock rates and turnaround offset

The proposed terrestrial flight experiment tests the proper-time history of a clock carried through matched powered ascent, ballistic turnaround, and matched powered descent. The rocket supplies momentum exchange through its exhaust, while Earth's ambient supplies the scale change associated with lifting. The calculation closes the idealized trajectory, propellant, and clock budgets. On this Einstein-equivalent branch, OQG's material-response description and GR's geometric representation give equivalent gravitational predictions.

Let z increase vertically upward from the departure station and let r be distance from Earth's center, with departure radius R_{E}. Thus $z=r-R_{\mathrm{E}}$ for radial flight. Let $\mu_{\mathrm{E}}=G_0M_{\mathrm{E}}$ be Earth's reference gravitational parameter, with M_{E} its mass. In the nonrotating Earth-only model, define $\Delta\Phi=\Phi-\Phi_0$, where Φ_0 is the departure potential. The natural scale and its outward gradient satisfy

$$\Delta\Phi(r)=\mu_{\mathrm{E}}\left(\frac{1}{R_{\mathrm{E}}}-\frac{1}{r}\right), \qquad \ln b\simeq\frac{\Delta\Phi}{c_0^2}$$
$$g(r)=\frac{\mathrm{d}\Phi}{\mathrm{d}r}>0, \qquad a_{\mathrm{ff}}=-g(r)\simeq-c_0^2\frac{\partial\ln b}{\partial z} \tag{49}$$

Here a_{ff} is the outward component of free-fall acceleration. The scale increases with altitude while gravity acts toward lower scale. The profile is inferred from terrestrial gravity; it is the natural ambient used to evaluate the material comparisons.

Let signed radial velocity be u=dz/dt. The weak-field limit of b=γ gives u^2=2$\Delta\Phi$. Differentiating along either moving branch fixes the required outward acceleration. With a_{thr} the thrust acceleration, the matching condition and flight equation give

$$u^2=2\Delta\Phi, \qquad \frac{\mathrm{d}u}{\mathrm{d}t}=+g(r)$$
$$\frac{\mathrm{d}u}{\mathrm{d}t}=a_{\mathrm{thr}}-g(r), \qquad a_{\mathrm{thr}}=2g(r) \tag{50}$$

One gravity of thrust balances the inward field, and the other supplies the outward acceleration required by the matched speed-versus-height relation. At this order an onboard accelerometer reads approximately $2g$. On descent, u is negative while the required acceleration remains outward, so the same thrust brakes the returning booster. A turnaround at positive altitude passes through u=0 with b>1, giving a calculable interval of clock-rate mismatch.

For a transparent benchmark, take constant g, neglect atmosphere and rotation, and use instantaneous thrust transitions. Let u_{c}>0 be cutoff speed, T=u_{c}/g the duration of each powered segment, and H=u_{c}^2/g the apogee height. Apply upward thrust acceleration $2g$ for time T, coast for $2T$, and apply upward $2g$ thrust for the final time T. The clock remains attached to the booster throughout. With s=t−T during coast and q=t−3T during landing, the trajectory is

$$z(t)=\begin{cases}\frac{1}{2}gt^2, & 0\le t\le T\\ \frac{1}{2}H+u_{\mathrm{c}}s-\frac{1}{2}gs^2, & 0\le s\le 2T\\ \frac{1}{2}H-u_{\mathrm{c}}q+\frac{1}{2}gq^2, & 0\le q\le T\end{cases} \tag{51}$$

The corresponding velocity is the derivative of each branch. Both powered intervals satisfy Eq. (50) to the retained weak-field order. Let τ_{B} and τ_{G} denote booster and ground proper time, set t=τ_{G}, and initialize their difference $\Delta\tau$=τ_{B}−τ_{G} to zero. During the first burn it remains zero. The coast fractional rate difference, ϵ_τ=d$\Delta\tau$/dt, is

$$\epsilon_\tau(s)\simeq\frac{gz(s)-u(s)^2/2}{c_0^2}=\frac{2gu_{\mathrm{c}}s-g^2s^2}{c_0^2} \tag{52}$$

This is positive between cutoff and landing-burn restart. At apogee the booster is momentarily stationary in the higher ambient, giving the largest rate difference. Integration yields

$$\Delta\tau_{\mathrm{coast}}(s)=\frac{gu_{\mathrm{c}}s^2-g^2s^3/3}{c_0^2}$$
$$\Delta\tau_{\mathrm{landing}}=\frac{4u_{\mathrm{c}}^3}{3gc_0^2} \tag{53}$$

The landing burn restores equal rates and retains the offset accumulated during coast. This explicit clock history distinguishes rate matching during propulsion from equality of readings over the entire round trip.

For H=100 km, g=9.81 m s^{-2}, and c_0=299792458 m s^{-1}, the cutoff speed is 990.454 m s^{-1}. Each burn lasts 100.964 s. The landing lead is 1.46937 ns, with half that value at apogee, and the maximum fractional rate difference is 1.09151×10^{-11}. Table 1 lists the events and Fig. 1 displays the trajectory and clock history. The quoted digits document the idealized arithmetic; an actual terrestrial trajectory requires a more complete environmental model.

Table 1 Events in the idealized 100 km vertical flight

Event	Time, s	Height, km	Velocity, m/s	Clock lead, ns
Start ascent	0.000	0.000	0.000	0.00000
End initial burn	100.964	50.000	+990.454	0.00000
Apogee	201.928	100.000	0.000	0.73469
Start landing burn	302.891	50.000	−990.454	1.46937
Touchdown	403.855	0.000	0.000	1.46937

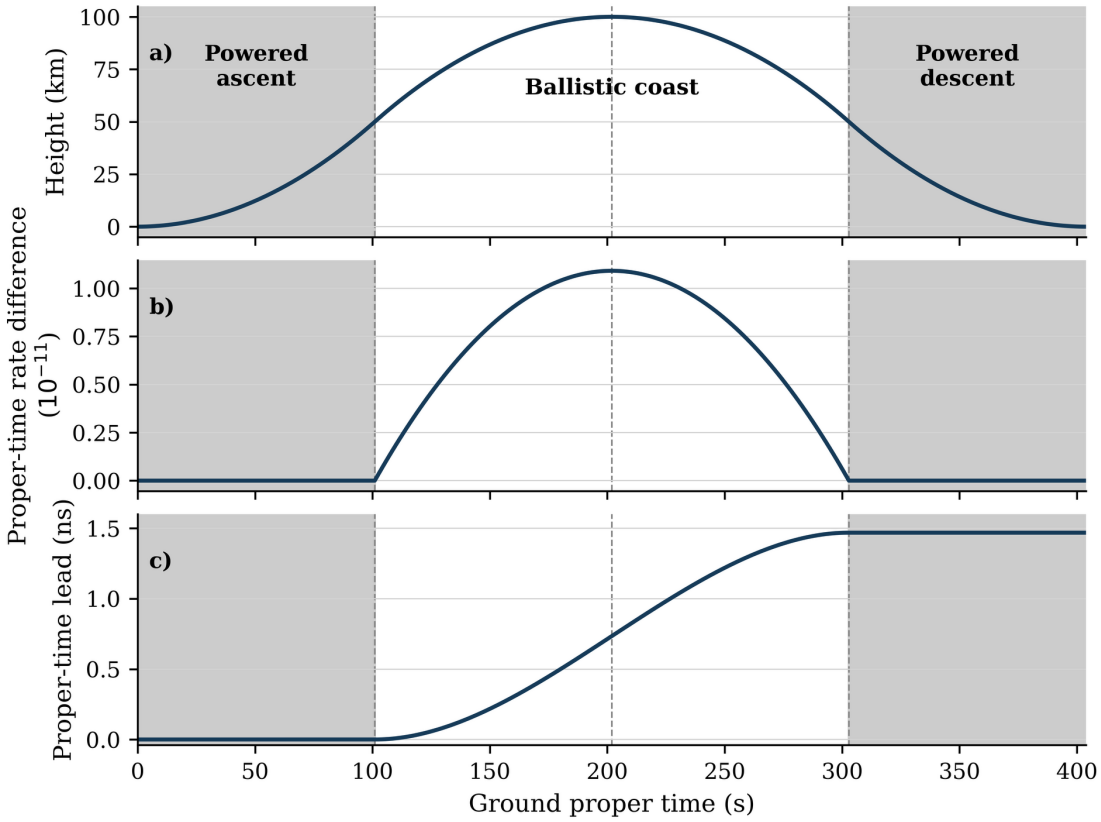


Fig. 1 Calculated height, fractional clock-rate difference, and booster clock lead. Shading marks the powered intervals; dashed lines mark cutoff, apogee, and landing-burn restart.

At the 50 km cutoff, $b-1 \simeq 5.45755\times10^{-12}$. The corresponding fractional increase in total stiffness and decrease in rest-state energy density each have leading magnitude 1.09151×10^{-11}. These are material ratios inferred from the specified OQG family. The clock comparison tests the proper-time history; an independent density measurement would test an additional observable.

The propulsion budget uses the time integral of thrust acceleration. Let F_{thr} be thrust force and m_{veh} instantaneous vehicle mass including remaining propellant. Each burn contributes $2u_{\mathrm{c}}$, so the total propulsive velocity increment is

$$\Delta v_{\mathrm{prop}} = \int \frac{|F_{\mathrm{thr}}|}{m_{\mathrm{veh}}}\,\mathrm{d}t = 4u_{\mathrm{c}} = 3.96182\ \mathrm{km\ s^{-1}} \tag{54}$$

For constant effective exhaust velocity v_{e}, let m_{i} and m_{f} be initial and final masses and I_{sp} specific impulse. The conventional standard gravity $g_{\mathrm{std}} = 9.80665\ \mathrm{m\ s^{-2}}$ defines specific impulse. The ideal rocket balance is

$$v_{\mathrm{e}} = g_{\mathrm{std}} I_{\mathrm{sp}}, \qquad \frac{m_{\mathrm{i}}}{m_{\mathrm{f}}} = \exp\left(\frac{\Delta v_{\mathrm{prop}}}{g_{\mathrm{std}} I_{\mathrm{sp}}}\right) \tag{55}$$

At an assumed $I_{\mathrm{sp}} = 450\ \mathrm{s}$, the mass ratio is 2.45411. Atmospheric drag, finite engine transitions, reserves, and vehicle hardware enter an actual mission budget. Propellant consumption is accounted separately from the

corresponding-state mass coefficient in Section VI. An artificial compensation system would add its source, hardware, and energy requirements.

Comparing separated clocks requires propagation corrections as well as the trajectory. Let $\mathcal{Z}$ denote received frequency divided by emitted frequency, each measured by its endpoint clock, and let the signed $\beta=u/c(r)$ use the booster velocity at the relevant event. For radial transfer in the static model, a matched segment gives

$$\mathcal{Z}_{\mathrm{G}\to\mathrm{B}}=\frac{\gamma(1-\beta)}{b}=1-\beta, \qquad \mathcal{Z}_{\mathrm{B}\to\mathrm{G}}=\frac{b}{\gamma(1+\beta)}=\frac{1}{1+\beta} \tag{56}$$

The uplink uses reception at the booster; the downlink uses emission there. These ratios retain Doppler shifts even during proper-time matching. Rocket-borne clock comparison with Doppler compensation has the experimental precedent of Gravity Probe A [30].

The proposed experiment combines a signal referenced to the flight clock with coherent two-way ranging or time transfer and independent trajectory data. A coherent returned echo measures propagation and motion; the clock-referenced signal supplies onboard phase. Recovery of the same clock permits a final integrated comparison, with calibrated transport included if touchdown differs from the reference location.

Let $\Delta\tau_{\mathrm{meas}}$ be the measured clock difference after intrinsic clock shifts are corrected. For a precision weak-field flight, use booster and ground potentials $\Phi_{\mathrm{B}},\Phi_{\mathrm{G}}$ and velocities $v_{\mathrm{B}},v_{\mathrm{G}}$ in one coordinate convention. Define the clock residual $\mathscr{R}_\tau$ by

$$\mathscr{R}_\tau(t)=\Delta\tau_{\mathrm{meas}}(t) -\frac{1}{c_0^2}\int_0^t\left[\Phi_{\mathrm{B}}(\vartheta)-\Phi_{\mathrm{G}}(\vartheta)-\frac{v_{\mathrm{B}}(\vartheta)^2-v_{\mathrm{G}}(\vartheta)^2}{2}\right]\mathrm{d}\vartheta \tag{57}$$

Earth rotation, external tidal potentials, the chosen geocentric time convention, and signal propagation must be included at the required precision. An accelerometer and environmental monitors on the clock plate record loading, vibration, temperature, and magnetic fields. The combined uncertainty should be sufficiently below the 1.46937 ns benchmark to resolve the full history and should also bound the rate residual during each burn. The terrestrial trajectory and its proper-time history follow the Einstein-equivalent branch, on which OQG's material-response description and GR's geometric representation give equivalent gravitational predictions. The proposed measurements test that common prediction through the residual in Eq. (57).

The longitudinal-length comparison is a separate metrology extension. At cutoff, a 10 m equilibrium ruler has an inferred ambient expansion of about 55 pm before the longitudinal kinematic cancellation. Testing that cancellation

requires simultaneous endpoint reconstruction and calibration of elastic and thermal strains. The worked flight establishes the central division quantitatively: thrust supplies the motion, the higher ambient supplies the matched material state, and the ballistic turnaround accumulates a lasting clock lead. An artificial generator must reproduce the required material history while carrying its own energy, reaction, and structural costs.

IX. The controller must track the accelerating vehicle and its own response

The onboard controller has a demanding physical job: supply the changing material state as the rocket accelerates the spacecraft. The preparation stores energy, changes binding, and must remain consistent across the generator, supports, sensors, and receiving matter. A single adjusted clock or a prescribed scale factor cannot establish that complete result. The target developed above now fixes the tracking law, increasing energy requirement, and spatial and mechanical checks that a candidate generator must satisfy.

Begin with the stationary internal state of Section IV and a desired scale $b(t)$. First hold the center of mass at rest relative to the reference. A dot denotes differentiation with respect to reference time t. Differentiating the unitary family gives a sufficient ideal tracking Hamiltonian H_{track} [31]:

$$H_{\mathrm{track}}(t)=H_{b(t)}+i\hbar\dot{U}_{b(t)}U_{b(t)}^{\dagger}=H_{b(t)}+\frac{\dot{b}}{b}D \tag{58}$$

The instantaneous stationary Hamiltonian commutes with its corresponding state. The counterdiabatic dilation term carries that state to the next member of the family. Its coefficient is the fractional scale rate. Once b is constant, this ideal closed-sector tracking term vanishes; maintenance power for an actual dissipative source remains in the complete budget. Equation (58) is the stationary preparation construction; motion changes the clock-phase generator as follows.

For the moving body, distinguish its total energy from the phase accumulated along its path. Let $\mathbf{p}_{\mathrm{cm}}$ be its center-of-mass canonical momentum, separate from the internal operator P, and let E_{phase} denote the coefficient of reference time in the along-path phase. For internal phases, prescribe the trajectory and compare corresponding clock levels at the same velocity. Let ${H_{\mathrm{path}}}^{(t)}$ denote their along-path phase generator in reference time t. Then

$$\begin{aligned} E_{\mathrm{mov}}&=\gamma E_b, \qquad \mathbf{p}_{\mathrm{cm}}=\gamma\frac{E_b}{c_b^2}\mathbf{u} \\ E_{\mathrm{phase}}&=E_{\mathrm{mov}}-\mathbf{p}_{\mathrm{cm}}\cdot\mathbf{u}=\frac{E_b}{\gamma} \\ {H_{\mathrm{path}}}^{(t)}(t)&=\frac{H_{b(t)}}{\gamma(t)}+\frac{\dot{b}}{b}D \end{aligned} \tag{59}$$

Evaluating $E_{\mathrm{mov}}dt - \mathbf{p}_{\mathrm{cm}} \cdot d\mathbf{x}$ along $d\mathbf{x} = \mathbf{u}dt$ gives the second line. A reference eigenstate accumulates the phase $\frac{E_n}{\hbar}\int [b(t)/\gamma(t)]dt$ while its internal spatial state follows $U_{b(t)}$. Differentiating that evolving state gives the third line, including the counterdiabatic term. Its clock gaps carry the factor b/γ. The along-path generator governs internal phase in this prescribed-trajectory approximation; total moving energy remains $E_{\mathrm{mov}} = \gamma E_b$ in the energy–momentum account.

Let V_{mov} and $\overline{\varepsilon}_{\mathrm{mov}}$ denote the simultaneous moving volume and its average total energy density. For a complete equilibrated body, with binding and support stresses included in its energy–momentum account,

$$V_{\mathrm{mov}}=\frac{b^3}{\gamma}V_0, \qquad \overline{\varepsilon}_{\mathrm{mov}}=\frac{E_{\mathrm{mov}}}{V_{\mathrm{mov}}}=\frac{\gamma^2}{b^2}\overline{\varepsilon}_0 \qquad \overline{\varepsilon}_{\mathrm{mov}}|_{b=\gamma}=\overline{\varepsilon}_0 \tag{60}$$

Motion contributes one longitudinal volume factor. At matching, the total moving energy and volume both increase by b^2, leaving their ratio unchanged. The prepared rest-state density remains lower by b^{-2}. Clock evolution uses the phase gap in Eq. (59); stress-energy density uses total energy and simultaneous volume.

The time history is fixed by the trajectory and the applicable propagation scale together. For one-dimensional motion with signed velocity u and reference acceleration a=du/dt, differentiating Eq. (9) gives

$$\frac{b}{\gamma}=1, \qquad \frac{\dot{b}}{b}=\frac{\dot{\gamma}}{\gamma}, \qquad \gamma=\left(1-\frac{u^2}{c_0^2 b^4}\right)^{-1/2} \qquad \frac{\dot{b}}{b}=\frac{ua}{c_0^2 b^2(2b^2-1)} \tag{61}$$

Increasing speed requires increasing compensation. On a slowing matched branch, the required scale decreases. The final expression supplies the controller's fractional-rate setpoint for a given matched trajectory. In the weak-scale limit it becomes $\dot{b}/b \simeq ua/c_0^2$.

The source must also establish a spatial history. Write $b_{\mathrm{s}}(t)=b(\mathbf{x}_{\mathrm{s}}(t),t)$ for the scale sampled at the spacecraft's reference point. The exact chain rule is

$$\frac{\mathrm{d}\ln b_{\mathrm{s}}}{\mathrm{d}t}=[\partial_t \ln b+\mathbf{u}\cdot\nabla \ln b]_{\mathbf{x}_{\mathrm{s}}(t)} \tag{62}$$

The scale change along the trajectory contains both local time variation and motion through a spatial gradient. In a stationary profile the first term vanishes. For an onboard source moving and accelerating with the ship, the solution must include the source history, propagation delay, boundaries, and the chosen simultaneity convention. Spatial uniformity at one time therefore specifies only part of the required field history. Increasing compensation

along an accelerating path must be included even when the intended instantaneous profile is uniform; the chain rule keeps that sampled change distinct from a spatial gradient at fixed time.

The work associated with the increasing scale can be expressed per distance traveled. Let x_s increase along one-dimensional motion and define $U_\mathrm{prep}=E_0(b_\mathrm{s}-1)$. At weak scale, for nonzero speed or its smooth limit from rest,

$$\frac{\mathrm{d}\ln b_\mathrm{s}}{\mathrm{d}x_\mathrm{s}}\simeq\frac{a}{c_0^2},\qquad \frac{\mathrm{d}U_\mathrm{prep}}{\mathrm{d}x_\mathrm{s}}\simeq M_0 a \tag{63}$$

These are derivatives along the actual trajectory. The second expression gives a positive preparation-work cost per distance during increasing-speed motion. This is the quantitative sense in which compensation is uphill. A mechanical resistance must additionally be obtained from the source–receiver coupling. If that solution produces a positive spatial gradient along travel, the weak-field force $-E_0\nabla b$ acts oppositely. Time-varying kinetic coefficients and field momentum enter the same force and power calculation.

An ideal homogeneous model shows the distinction explicitly. Let $\mathscr{H}$ denote the translational Hamiltonian, expressed in center-of-mass momentum and a prescribed spatially uniform $b(t)$. Eliminating velocity from Eq. (59) gives

$$\begin{gathered}\mathscr{H}(\mathbf{p}_\mathrm{cm},b)=\sqrt{E_0^2b^2+c_0^2b^4|\mathbf{p}_\mathrm{cm}|^2}\\ \frac{\mathrm{d}\mathscr{H}}{\mathrm{d}t}=\mathbf{u}\cdot\dot{\mathbf{p}}_\mathrm{cm}+E_0(2\gamma-\gamma^{-1})\dot{b}\end{gathered} \tag{64}$$

Here $\mathbf{u}=\partial\mathscr{H}/\partial\mathbf{p}_\mathrm{cm}$ and $\gamma=\mathscr{H}/(E_0b)$. The first term is mechanical power in this model; the second is generalized control power at fixed momentum. On the one-dimensional matched family they become $E_0\dot{b}/b$ and $E_0(2b-b^{-1})\dot{b}$, respectively. Their sum is $2E_0b\dot{b}$, the derivative of the total energy in Eq. (28). The prescribed-field model identifies the terms that a physical source must supply. Its realization must also account for the generator's own force, energy change, and field momentum.

A finite spacecraft introduces variation among clocks and structures. For a calibrated material standard labeled j, let b_j and γ_j be its local scale and motion factors in the declared reference comparison. Define its logarithmic clock-rate error η_j and a small variation $\delta\eta_j$ by

$$\eta_j=\ln\left(\frac{b_j}{\gamma_j}\right),\qquad \delta\eta_j=\delta\ln b_j-\delta\ln\gamma_j \tag{65}$$

Feedback must bound both the common error and differences between standards after signal propagation and intrinsic clock shifts are corrected. Different positions in an accelerating body can have different velocity and clock

comparisons. The generator's own response belongs in that map. If the generator remains at one preparation while the payload is driven to another, their boundary must accommodate the resulting differences in equilibrium dimensions, spectra, and mechanical response. An interface can carry traction, strain, and thermal mismatch; their values follow from the actual coupling and material boundary conditions. Any repulsive force on the payload also loads the source and its fields according to Eq. (3). Structural design must carry that reaction while the controller maintains the clock comparison.

Source resources also change during operation. Battery discharge, fuel conversion, and propellant consumption alter composition or state separately from fixed-content scaling. A physical controller must distinguish its prepared hardware from these changing reservoirs and retain reference state 0 as the external comparison. Table 2 collects the resulting outputs and checks.

Table 2 Controller outputs and verification requirements

Output	Required comparison or check
Internal spatial pattern	Corresponding wavelengths, interference intervals, and equilibrium lengths scale by b
Momentum and binding spectrum	Internal components and gaps scale by b^{-1}; transition gaps scale by b; binding and covariance remain compatible
Complete rest state	Energy scales by b, volume by b^3, density by b^{-2}, and total spectral stiffness by b^2
Dynamic tracking	Scale and fractional scale rate follow Eq. (61) over the required bandwidth
Spatial clock agreement	The common value and spatial differences of η_j remain within the specified tolerances
Generator and structure	Source, payload, sensors, and supports have calculated responses, interface tractions, and stable material states
Full operating budget	Source power, propulsion, field momentum, radiation, losses, and consumed resources close one energy–momentum balance

To connect these outputs to apparatus inputs, let $f_\alpha(t)$ denote controllable source parameters, with α labeling control channels. Let $H_{\text{eff}}[f]$ and ρ_{eff} be the effective generator of internal phase along the prescribed trajectory in reference time and the resulting state. Using the same-velocity clock comparison of Eq. (59), the ideal implementation target is

$$H_{\text{eff}}[f(t)] \simeq \frac{H_{b(t)}}{\gamma(t)} + \frac{\dot{b}}{b} D$$
$$\rho_{\text{eff}}(t) \simeq U_{b(t)} \rho_0 U_{b(t)}^{\dagger} \tag{66}$$

At rest, $\gamma = 1$ and the first line reduces to Eq. (58). The approximations express finite control accuracy measured through the observables; environmental coupling and noise extend the description for an open quantum system. This phase-generator target does not replace the total-energy budget. The source inputs must realize the common binding Hamiltonian and its counterdiabatic tracking across the relevant matter.

For a first local assessment, let y_i be logarithmic changes of selected positive observables and let Ω be control modulation angular frequency. Define the retarded response matrix $M_{i\alpha}^{R}(\mathbf{x},\mathbf{x}';\Omega)$ to relate an input at source position $\mathbf{x}'$ to output i at $\mathbf{x}$. Small changes obey

$$\delta y_i(\mathbf{x},\Omega) = \sum_\alpha \int \mathrm{d}^3x'\, M_{i\alpha}^{R}(\mathbf{x},\mathbf{x}';\Omega)\delta f_\alpha(\mathbf{x}',\Omega) \tag{67}$$

For ordered outputs $\left(\ell_{12},|\delta p_{12}|,\Delta E_{\mathrm{tr}},V_b,\bar{\varepsilon}_b,A_{2,\mathrm{E}}^{\mathrm{tot}}\right)$, the common-scale direction is $(1,-1,1,3,-2,2)\delta\ln b$. The source must reach this linked direction with compatible correlations and stable binding. Spatial dependence tests uniformity and hardware participation, while the frequency response tests bandwidth and delay. Finite preparations require the response beyond the initial linear neighborhood.

Finally, choose a boundary containing the vehicle, its onboard source, interacting fields, and supports. Let E_{veh}, E_{src}, and E_{int} denote the corresponding energy contributions, counted once; E_{veh} includes translation. Let P_{in} and P_{out} be total incoming and outgoing boundary power, including mechanical work, field and radiation transfer, and material transport; let $\mathbf{F}_{\mathrm{ext}}$ be an externally applied force, and $\mathbf{J}_{P,\mathrm{in}}$, $\mathbf{J}_{P,\mathrm{out}}$ incoming and outgoing momentum rates. Then

$$\begin{aligned} \frac{\mathrm{d}}{\mathrm{d}t}\left(E_{\mathrm{veh}}+E_{\mathrm{src}}+E_{\mathrm{int}}\right) &= P_{\mathrm{in}}-P_{\mathrm{out}} \\ \frac{\mathrm{d}\mathbf{P}_{\mathrm{tot}}}{\mathrm{d}t} &= \mathbf{F}_{\mathrm{ext}}+\mathbf{J}_{P,\mathrm{in}}-\mathbf{J}_{P,\mathrm{out}} \end{aligned} \tag{68}$$

Each interaction is represented either within the boundary or as a transfer across it. The ideal rest-state preparation rate is $\dot{E}_b = E_0\dot{b}$; source losses, recoil, and changing resources complete the account. Ordinary thrust loading remains a separate requirement from matched clock rates. A source intended also to alter passenger acceleration must establish that result through the spatial force balance and support response. Boundary power includes work by external forces. Each transfer enters once, and gravitational potential energy already assigned through E_b is not added again as a separate energy term.

A claimed propulsive signal must be measured on the complete apparatus. The recommended thrust-measurement practice of Polk et al. [32] supplies an experimental starting point: calibrate the installed balance with

known forces, repeat calibrations around operation, quantify uncertainty, and evaluate thermal drift, electromagnetic coupling, cable and plumbing forces, and gas flow. For a candidate generator, the measured boundary must also account for radiated momentum and any external support. A force between payload and source is an internal load; the experiment must resolve the net force on the assembly. Reversing the proposed force direction and repeating controlled null runs can further test apparatus-specific artifacts.

The controller's deliverable is a stable, spatially consistent bound-state preparation that follows $b = \gamma$, with stored energy, source reaction, losses, and changing resources accounted for. Its measured clocks and equilibrium dimensions must meet the linked targets; any proposed change in passenger acceleration also requires the spatial force and support calculation.

X. Conclusion

Spacetime constructs are inadmissible as independent physical propulsion mechanisms in OQG. On its selected Einstein-equivalent branch, geometry organizes the clock and ruler comparisons produced by matter and its retarded stress response. The complete-system conservation result separately establishes the propulsion boundary: an isolated ship and controller in a uniform exterior cannot accelerate through internal stresses. The generator, power supply, supports, and fields participate in every reaction. Exhaust, radiation, and external bodies provide explicit momentum-transfer channels, with radiation-only recoil bounded by the ideal photon-rocket value. These results identify the physical source and reaction that any proposed drive must supply.

Within the stated OQG family, covariant material scaling stores gravitational lifting work in the body's bound state. Measured in retained external standards, reversible lifting work equals the increase in bound-state energy. For reference bound-state energy E_0 and material scale factors b_1 and b, the stored increase is $E_0(b - b_1)$. This is the assigned gravitational potential-energy increase, counted once. Rest energy scales by b, equilibrium volume by b^3, and positive rest-state energy density by b^{-2}. The quantum-state construction specifies the coordinated change of spatial patterns, transition energies, and binding that carries this stored work. Greater stored energy and lower density are linked consequences of the same preparation.

The matched-state condition $b = \gamma$, where γ is the Lorentz factor, gives equal proper-time rates and restores the longitudinal reference length. With speed u, Newtonian potential rise $\Delta\Phi$, local gravity g, and outward thrust acceleration a_{thr}, the weak-field radial trajectory obeys $u^2 = 2\Delta\Phi$ and $a_{\mathrm{thr}} = 2g$. The proposed 100 km terrestrial

flight experiment tests these matched powered branches relative to the ground clock using Earth's ambient and conventional thrust. Ballistic turnaround produces a 1.46937 ns lead retained at landing. The propulsive velocity increment is 3.96182 km/s, with ideal mass ratio 2.45411 at 450 s specific impulse. The complete clock history distinguishes equal rates during powered motion from the accumulated turnaround offset on the Einstein-equivalent branch. OQG and GR give equivalent gravitational predictions for this history; the proposed measurements test the matched burn rates and accumulated coast offset.

The resulting controller specification ties the material scale to an ideal tracking Hamiltonian, a preparation-energy requirement, and linked measurements of spectra, dimensions, density, and stress response. It includes the generator's participation, interface tractions, and complete energy–momentum budget. The paper thereby turns the material-control objective into quantitative preparation and measurement criteria alongside a proposed flight experiment with a calculated trajectory and clock history. Matter tells matter how to scale. Geometry is just bookkeeping.

Acknowledgments

This work was self-funded. The author declares no conflict of interest.

The author used OpenAI ChatGPT and Codex for literature organization, assistance with mathematical derivations and consistency checks, preparation of Python verification scripts, manuscript drafting and assembly, and language editing. The author is responsible for the scientific content, source attribution, and final manuscript.

References

[1] Desiato, T. J., "Operational Quantum Gravity in Practice: Spectral Stiffness, Matter Scaling, Equivalence, and Cosmology without Dark Energy," preprint, Version 0.3, 2026. https://www.academia.edu/175371020.

[2] Desiato, T. J., "Operational Quantum Gravity: From a Standard-Model Stress Hessian to Einstein-Equivalent WTDiff Dynamics," preprint, Version 0.3, 12 September 2026. https://www.academia.edu/175443563.

[3] Desiato, T. J., "Operational Quantum Gravity: From Standard Model Stress Response to Gravity-Induced Entanglement," preprint, Version 0.5, 17 September 2026. https://www.researchgate.net/publication/414425911.

[4] Alcubierre, M., "The Warp Drive: Hyper-Fast Travel within General Relativity," *Classical and Quantum Gravity*, Vol. 11, No. 5, 1994, pp. L73–L77. https://doi.org/10.1088/0264-9381/11/5/001.

[5] Natário, J., "Warp Drive with Zero Expansion," *Classical and Quantum Gravity*, Vol. 19, No. 6, 2002, pp. 1157–1165. https://doi.org/10.1088/0264-9381/19/6/308.

[6] Santiago, J., Schuster, S., and Visser, M., "Generic Warp Drives Violate the Null Energy Condition," *Physical Review D*, Vol. 105, No. 6, 2022, Article 064038. https://doi.org/10.1103/PhysRevD.105.064038.

[7] Millis, M. G., "Challenge to Create the Space Drive," *Journal of Propulsion and Power*, Vol. 13, No. 5, 1997, pp. 577–582. https://ntrs.nasa.gov/citations/19980021277.

[8] Desiato, T. J., "The Electromagnetic Quantum Vacuum Warp Drive," *Journal of the British Interplanetary Society*, Vol. 68, 2015, pp. 347–353. https://bis-space.com/shop/product/the-electromagnetic-quantum-vacuum-warp-drive/.

[9] Tong, D., *General Relativity*, lecture notes, University of Cambridge, Cambridge, England, U.K., 2019, Chap. 4, Secs. 4.3.2 and 4.5.5. https://davidtong.org/teaching/general-relativity/grhtml/S4.

[10] Szabados, L. B., "Quasi-Local Energy-Momentum and Angular Momentum in General Relativity," *Living Reviews in Relativity*, Vol. 12, No. 1, 2009, Article 4. https://doi.org/10.12942/lrr-2009-4.

[11] Fewster, C. J., "Lectures on Quantum Energy Inequalities," 2012. arXiv:1208.5399.

[12] Bobrick, A., and Martire, G., "Introducing Physical Warp Drives," *Classical and Quantum Gravity*, Vol. 38, No. 10, 2021, Article 105009. https://doi.org/10.1088/1361-6382/abdf6e.

[13] Fuchs, J., Helmerich, C., Bobrick, A., Sellers, L., Melcher, B., and Martire, G., "Constant Velocity Physical Warp Drive Solution," *Classical and Quantum Gravity*, Vol. 41, No. 9, 2024, Article 095013. https://doi.org/10.1088/1361-6382/ad26aa.

[14] Zwiebach, B., "Particle Nature of Light and Wave Nature of Matter," *Quantum Physics I*, Massachusetts Institute of Technology OpenCourseWare, Lecture 3, 16 February 2016, Sec. 3. https://ocw.mit.edu/courses/8-04-quantum-physics-i-spring-2016/f928b8dce3d6a218fddda9617c5eb4f2_MIT8_04S16_LecNotes3.pdf.

[15] Zwiebach, B., *Quantum Physics I*, Massachusetts Institute of Technology OpenCourseWare, Spring 2016, Lectures 7 and 8, "Wavepackets and Uncertainty" and "Uncovering Momentum Space." https://ocw.mit.edu/courses/8-04-quantum-physics-i-spring-2016/pages/lecture-notes/.

[16] Desiato, T. J., "Operational Quantum Gravity: Canonical Scale Covariance and the Zero-Extension Boundary of Black-Hole Matter," preprint, Version 0.3, 6 September 2026. https://www.researchgate.net/publication/414035039.

[17] Tong, D., *Quantum Field Theory*, lecture notes, University of Cambridge, Cambridge, England, U.K., 2006, Secs. 2 and 5. https://www.damtp.cam.ac.uk/user/tong/qft.html.

[18] Tong, D., *Gauge Theory*, lecture notes, University of Cambridge, Cambridge, England, U.K., 2018, Sec. 2.2.1. https://www.damtp.cam.ac.uk/user/tong/gaugetheory.html.

[19] Burkert, V. D., Elouadrhiri, L., Girod, F. X., Lorcé, C., Schweitzer, P., and Shanahan, P. E., "Colloquium: Gravitational Form Factors of the Proton," *Reviews of Modern Physics*, Vol. 95, No. 4, 2023, Article 041002. https://doi.org/10.1103/RevModPhys.95.041002.

[20] Ekström, A., Hagen, G., Morris, T. D., Papenbrock, T., and Schwartz, P. D., "Delta Isobars and Nuclear Saturation," *Physical Review C*, Vol. 97, No. 2, 2018, Article 024332. https://doi.org/10.1103/PhysRevC.97.024332.

[21] Milonni, P. W., *The Quantum Vacuum: An Introduction to Quantum Electrodynamics*, Academic Press, San Diego, CA, 1994, Sec. 3.3.

[22] Puthoff, H. E., "Quantum Ground States as Equilibrium Particle–Vacuum Interaction States," 2012. arXiv:1204.1952.

[23] Ford, G. W., Lewis, J. T., and O'Connell, R. F., "Quantum Langevin Equation," *Physical Review A*, Vol. 37, No. 11, 1988, pp. 4419–4428. https://doi.org/10.1103/PhysRevA.37.4419.

[24] Callen, H. B., and Welton, T. A., "Irreversibility and Generalized Noise," *Physical Review*, Vol. 83, No. 1, 1951, pp. 34–40. https://doi.org/10.1103/PhysRev.83.34.

[25] Schwinger, J., "Brownian Motion of a Quantum Oscillator," *Journal of Mathematical Physics*, Vol. 2, No. 3, 1961, pp. 407–432. https://doi.org/10.1063/1.1703727.

[26] Keldysh, L. V., "Diagram Technique for Nonequilibrium Processes," *Soviet Physics Journal of Experimental and Theoretical Physics*, Vol. 20, No. 4, 1965, pp. 1018–1026.

[27] Desiato, T. J., "Static Transverse-Traceless Stress Susceptibility of the High-Temperature Standard Model through Second Order in the Couplings," preprint, Version 0.4, 11 September 2026. https://www.academia.edu/175443540.

[28] Álvarez, E., Blas, D., Garriga, J., and Verdaguer, E., "Transverse Fierz–Pauli Symmetry," *Nuclear Physics B*, Vol. 756, No. 3, 2006, pp. 148–170. https://doi.org/10.1016/j.nuclphysb.2006.08.003.

[29] Álvarez, E., and Vidal, R., "Weyl Transverse Gravity and the Cosmological Constant," *Physical Review D*, Vol. 81, No. 8, 2010, Article 084057. https://doi.org/10.1103/PhysRevD.81.084057.

[30] Vessot, R. F. C., Levine, M. W., Mattison, E. M., Blomberg, E. L., Hoffman, T. E., Nystrom, G. U., Farrel, B. F., Decher, R., Eby, P. B., Baugher, C. R., Watts, J. W., Teuber, D. L., and Wills, F. D., "Test of Relativistic Gravitation with a Space-Borne Hydrogen Maser," *Physical Review Letters*, Vol. 45, No. 26, 1980, pp. 2081–2084. https://doi.org/10.1103/PhysRevLett.45.2081.

[31] Deffner, S., Jarzynski, C., and del Campo, A., "Classical and Quantum Shortcuts to Adiabaticity for Scale-Invariant Driving," *Physical Review X*, Vol. 4, No. 2, 2014, Article 021013. https://doi.org/10.1103/PhysRevX.4.021013.

[32] Polk, J. E., Pancotti, A., Haag, T., King, S., Walker, M., Blakely, J., and Ziemer, J., "Recommended Practice for Thrust Measurement in Electric Propulsion Testing," *Journal of Propulsion and Power*, Vol. 33, No. 3, 2017, pp. 539–555. https://doi.org/10.2514/1.B35564.